- Technical Paper -

INVESTIGATING THERMAL EFFECTS ON THE CHARACTERISTICS OF CALCIUM OXIDE FROM SEA SHELL WASTE

Novik KUROHMAN[1], Heesup CHOI[2], Masumi INOUE[3] and Masato KIDA[4]

ABSTRACT

Marine waste is abundant in $CaCO_3$ and can be converted into CaO through calcination. Scallops, oysters, and clam shells from Hokkaido, Japan, were chosen for their abundance. The traditional calcination practice of seashells often involves uncontrolled heating at excessively high temperatures, leading to high energy consumption and CO_2 emissions. This study aims to reduce energy consumption by identifying an optimal calcination temperature that avoids overheating, thereby minimizing environmental impact. XRD and TG-DTA confirmed the complete conversion of $CaCO_3$ to CaO, while FT-IR indicated functional group changes, and NMR identified the crystalline forms of uncalcined $CaCO_3$.

1. INTRODUCTION

Globally, the fishery industry is projected to grow due to the increased demand for fishery expenditure. In Japan, the annual production of scallop farming reached around 500 thousand tons, with a total value of approximately 84 billion JPY (about 840 million USD) [1]. Approximately 60 % of sea shell waste products come from Hokkaido, particularly the Okhotsk Sea and Funka Bay [2]. Furthermore, inadequate sea shell waste management poses significant environmental challenges, including soil contamination. Without proactive countermeasures, these pressing issues are likely to worsen considerably.

Calcium carbonate ($CaCO_3$) derived from marine organisms can be transformed into calcium oxide (CaO) through calcination. This thermal decomposition occurs at high temperatures below the melting point and does not require chemicals [3]. Furthermore, CaO derived from sea shell waste offers potential for various applications, such as cement and fine aggregate replacement [4].

While previous studies have primarily focused on using seashell waste as a material replacement, this research delves deeper into its untapped potential as a valuable source of CaO for cementitious materials. Notably, the novel integration of multiple analytical techniques, including XRD, FT-IR, NMR, and TG-DTA, provides a more precise evaluation of thermal effects than earlier approaches.

The traditional calcination practice of seashells often involves uncontrolled heating at excessively high temperatures, leading to high energy consumption and CO_2 emissions. This study aims to reduce energy consumption by identifying an optimal calcination temperature that avoids overheating, thereby minimizing environmental impact. This approach also promotes a more sustainable method for producing CaO.

Unlike traditional methods that focus solely on high-temperature calcination, this study examines how calcination temperature affects the functional properties of CaO. The results highlight the improvements in energy efficiency and material quality, emphasizing the innovative approach of this method.

To achieve these objectives, the mineralogical composition of $CaCO_3$ polymorphs from sea shell waste was analyzed using microanalysis techniques such as X-ray diffraction (XRD) and Nuclear Magnetic Resonance (NMR), which enable detailed characterization of the structural and compositional transformations of $CaCO_3$ polymorphs. Fourier-transform infrared spectroscopy (FT-IR) was employed to investigate changes in functional groups under different calcination conditions. Similarly, thermogravimetric analysis (TG-DTA) was used to assess the thermal decomposition behavior of the samples under different temperatures.

By identifying optimal calcination conditions and the characteristics of sea shells, this research contributes to developing eco-friendly building materials while also helping to reduce sea shell waste in Japan.

2. MATERIALS AND METHODS

2.1 Materials

Waste shells of scallop shells *(Pecten maximus*), oyster shells (*Crassostrea belcheri*), and clam shells (*Ruditapes philippinarum*) were collected in Kitami, Hokkaido, Japan. The selection of the samples is due to their widespread availability and abundance in the region. The sea shells waste were rinsed and cleaned to remove surface impurities and salts. Subsequently, the cleaned samples were dried in an oven at 105°C for 24

*1 Graduate Student, Faculty of Engineering, Kitami Institute of Technology, JCI Student Member
*2 Prof., Department of Social and Environmental Sciences, Kitami Institute of Technology, JCI Member
*3 Prof., Department of Social and Environmental Sciences, Kitami Institute of Technology, JCI Member
*4 Associate Prof., School of Earth, Energy and Environmental Engineering, Kitami Institute of Technology

hours to eliminate residual moisture and organic substances and then placed in the vacuum chamber. The vacuum chamber protects them from contamination and moisture absorption. The obtained powder was then stored in a vacuum chamber to preserve its stability until subsequent use.

(1) Preparation of calcined powder

The cleaned shells were heated in an electric furnace (Yamamoto, Japan) at three distinct temperatures (650 ºC 750 ºC, and 850 ºC) for 8 hours. Afterward, the shells were manually ground with a ceramic grinder and sieved through a 100 µm mesh.

(2) Preparation of uncalcined powder

The uncalcined shells were manually ground using a ceramic grinder and sieved through a 100 µm mesh. The prepared powders were securely stored in a vacuum chamber to ensure purity and prevent moisture absorption.

2.2 Methods

(1) FT-IR

Functional groups in the samples were identified using an FT-IR 4700 spectrometer (JASCO), scanning a wavenumber range of 400–4000 cm^{-1}. The results were recorded as percentage transmission (%T) to detect shifts in functional groups caused by calcination.

(2) XRD analysis

The chemical shifts and crystal structures, both pre-and post-calcination samples, were analyzed using an X-ray Diffractometer (Ultima IV, Bruker, Germany) equipped with CuKα radiation operating at 40 kV and 20 mA. The scans were performed over a 2θ range of 5° to 65° at a speed of 2° per minute.

(3) TG-DTA

Thermal decomposition properties were examined using a TG-DTA system (Thermo Plus, Rigaku, Japan) under a nitrogen (N_2) atmosphere at a 10 °C/min heating rate. Approximately 15 mg of each sample, calcined and uncalcined, was tested. The TG-DTA analysis provided detailed information on weight loss patterns, the thermal decomposition of $CaCO_3$ into CaO, and the release of CO_2.

(4) NMR analysis

Solid-state NMR spectroscopy was performed using a Bruker ULTRASHIELD 400 WB PLUS spectrometer, operating at the resonance frequency of 100 MHz for carbon nuclei. Magic angle spinning (MAS) was employed for all solid-state measurements of 10000 Hz in a 4 mm rotor.

Further, for the 13C MAS NMR spectra, proton direct excitation was achieved using a single 90° pulse of 5.0 µs duration. The fully decoupled free induction decay (FID) was acquired over 160 to 212 scans, and then Fourier transformed to generate the corresponding line spectrum. A relaxation period of 540 seconds was incorporated between experiments to ensure complete spin-lattice relaxation. All experiments were conducted at atmospheric temperature [5].

3. DISCUSSIONS

3.1 FT-IR results

The FTIR spectra of heat-treated scallop shells were categorized by various band spectrums from 500 to 4000 cm^{-1}. Predominantly, the heated treatment may influence the IR spectrum. The peaks diminished and broadened with increasing temperatures.

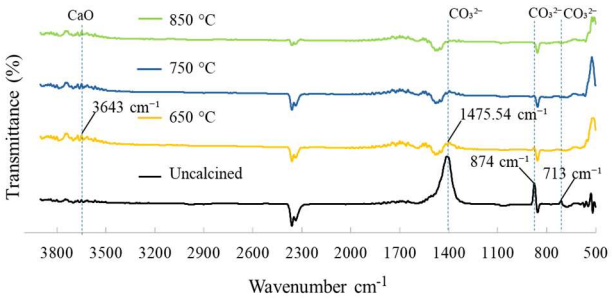

Fig.1 Results of FT-IR scallop shell

Fig.1 and Table 1 showed the bands at 713 cm^{-1} and 874 cm^{-1} disappeared at higher temperatures, demonstrating the absence of carbonate as $CaCO_3$ decomposed into CaO. As the temperature increased, a slight absorption band at 3643 cm^{-1} emerged, corresponding to Ca–O stretching. FT-IR enables the monitoring of $CaCO_3$ decomposition into CaO at high temperatures, with the broadening of the 1475.54 cm^{-1} peak signaling the breakdown of CO_3^{2-} and CO_2 during thermal decomposition. Overall, thermal treatment significantly influenced the IR spectrum, as demonstrated by the disappearance of specific peaks and the broadening of the spectrum at elevated temperatures.

Scallop shells were chosen for FT-IR test due to their abundance as a seafood industry byproduct in Hokkaido, making them sustainable and cost-effective material. The $CaCO_3$ content, predominantly in calcite Fig.2 (a), along with its stable rhombohedral structure, makes scallop shells ideal for studying $CaCO_3$ polymorphs. Further, calcite offers excellent stability under heating treatments, providing a reliable basis for experimental results [6].

FT-IR analysis identifies functional groups and confirms distinct $CaCO_3$ phases through characteristic vibrational bands, complementing XRD and NMR by providing molecular-level insights into chemical bonding. However, the FT-IR measurement did not resolve significant changes associated with temperatures. Therefore, it will be further elucidated in subsequent sections using XRD and NMR techniques for a more detailed analysis.

Table 1 List of the FTIR spectrums for scallop shell (Modified from [7])

FTIR results (cm^{-1})	Assignments (v)	Ref.
3643	Ca-O stretching	[8][9]
1475.54, 1411	CO_3^{2-} stretching	[10]
874	CO_3^{2-} (out-of-plane bending)	[11]
713	CO_3^{2-}(in-plane bending)	[12]

3.2 XRD results

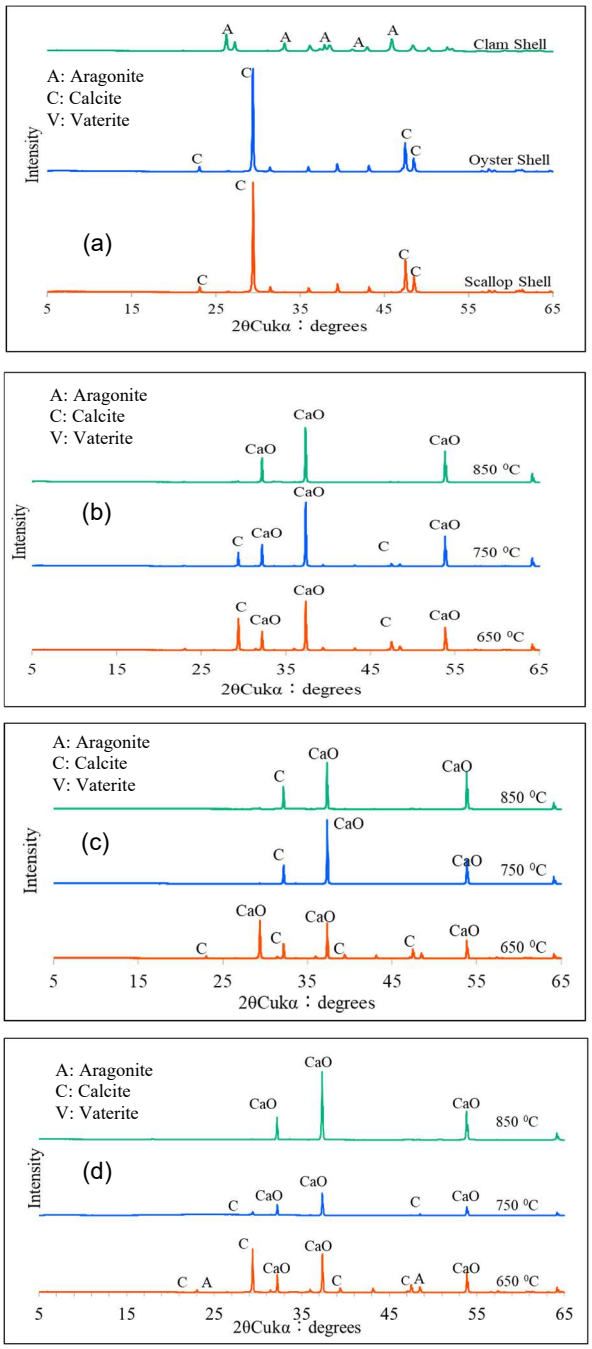

Fig.2 XRD Results for (a) uncalcined sea shells (b) calcined scallop shell (c) calcined oyster shell and (d) calcined clam shell

Fig.2 (a) presents the XRD patterns of uncalcined samples with a 2θ range of 5° to 65°. For the unheated scallop and oyster shells, diffraction peaks corresponding to calcite were predominantly observed at 23.1°, 29.39°, 36.0°, 47.5°, and 48.5° reflecting that the primary phase is calcite. Further, the diffraction peaks of the clam shells corresponded to aragonite, with notable peaks at 26.2°, 26.3°, 38.0°, 43.2° and 45.9°. As the temperature increased in Fig.2 (b), (c), and (d), new peaks appeared at 37.12° and 53.80°, indicating the presence of CaO. This illustrates the variation in mineralogical compositions before and after calcination.

The stability of calcite at 750 °C, as shown in Fig. 2 (b), (c), and (d), may result from a complex interaction of thermodynamic and kinetic factors. Calcite possesses a more stable rhombohedral structure [13]. Notably, the persistence of calcite at 750 °C, can be attributed to kinetic stabilization mechanisms. These mechanisms, including impurities and nanoparticle effects, inhibit the phase transformation, thereby maintaining the calcite structure. Recent studies have expanded on this, demonstrating that impurities like Mg^{2+}, SO_4^{2}, and organic molecules adsorb on crystal surfaces, disrupting the energy balance required for transformation [14].

Equally important, from a thermodynamic perspective, the complete conversion of $CaCO_3$ to CaO at 850 °C occurred due to several key factors. At 850°C (1123 K), the decomposition of $CaCO_3$ becomes thermodynamically spontaneous as the standard Gibbs free energy change ($\Delta G°$) turns negative, favoring the formation of CaO and CO_2. The reaction is endothermic (Fig.5) with value enthalpy change ($\Delta H° = 177.8$ kJ/mol), which requires a heat input, but this is offset by a substantial increase in entropy ($\Delta S° = 160.5$ J/K·mol), driven primarily by the release of gaseous CO_2 [15]. In addition, at 850°C, $CaCO_3$ decomposes rapidly, with CO_2 released at pressures above atmospheric, driving the reaction to completion.

It can be concluded from XRD that the complete decomposition of $CaCO_3$ to CaO occurs at 850°C, which facilitates enhanced reactivity and improved microstructural properties. However, further investigation using TG-DTA is necessary to determine the Optimum Degradation Temperature (ODT) precisely, thereby identifying the most optimal temperature for the degradation of $CaCO_3$. Also, the data from Fig.2, highlighted distinct mineralogical peaks and thermal behavior patterns, offering valuable insights into the strengths and limitations of each shell type for material selection.

3.3 TG-DTA results

The TGA patterns in Fig.3 showed similar behavior, and each weight loss can be divided into three general steps in Table 2 [16]. The first up to 125 °C could be attributed to the release of residual (0.1–0.15%) adsorbed moisture. The second decomposition step, occurring between approximately 125°C and 550°C, corresponds to the release of organic matter in the sea shells. The weight loss during this stage varies, with 1.80 % for scallop shells, 1.9 % for oyster shells, and 1.85 % for clam shells.

Besides, the primary weight loss, associated with the decomposition of $CaCO_3$, occurred between 550 °C and 795 °C and was attributed to the release of CO_2. [11]. During the primary stage, the weight loss also differs, with scallop shells losing weight loss 46.21 %, oyster shells 47.11 %, and clam shells 43.15, respectively.

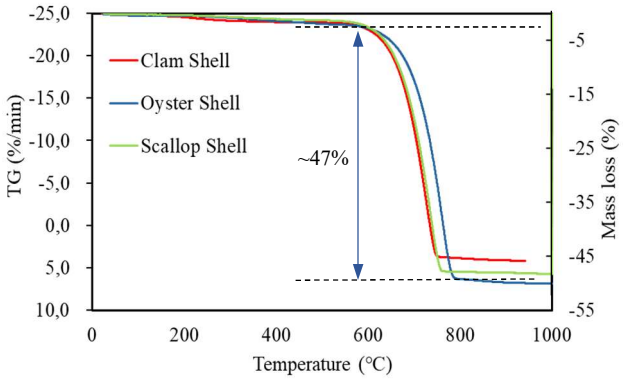

Fig.3 TGA Results for uncalcined sea shells

Table 2 Weigh losses in TGA of uncalcined samples

Raw Sample	Weight loss			
	Moisture (%)	Organic matter (%)	CO_2 (%)	Total (%)
	20-125 °C	125-550 °C	550-795 °C	20-1000 °C
Scallop Shell	0,10	1,80	46,21	48,20
Oyster Shell	0,10	1,90	47,11	50,00
Clam Shell	0,15	1,85	43,15	46,00

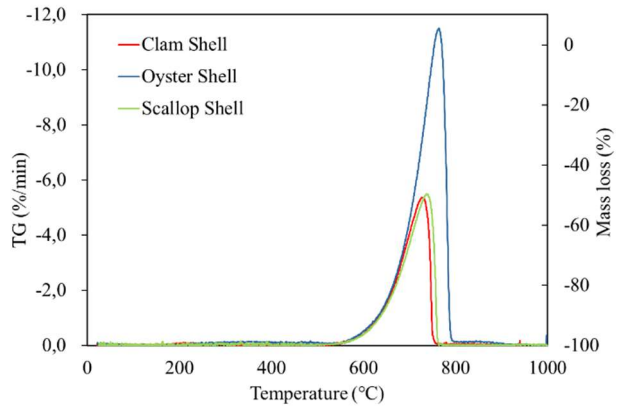

Fig.4 DTG Results for uncalcined sea shells

Meanwhile, Fig.4 shows the Optimum Degradation Temperatures (ODT) for scallop, clam, and oyster shells were approximately 740 °C, 730 °C, and 750 °C, respectively. ODT represents the temperature at which $CaCO_3$ undergoes its most rapid decomposition [17]. Oyster shells demonstrated a pronounced peak in the 550-800 °C temperature range, indicating a fast and intense mass loss. This behavior is driven by a highly endothermic decomposition process that requires substantial energy to disrupt chemical bonds [18]. In contrast, the scallop shell decomposes at around 550 °C, with complete calcination occurring at 770 °C. Similarly, the clam shells started to decompose at 550 °C until reaching completion at 750 °C, which displays a lower peak than oyster shells, corresponding to a slower decomposition process.

This slower and less intense mass loss in scallop and clam shells reflects lower energy requirements for decomposition. Also, the differences in thermal behavior between oysters, scallops, and clam shells might be influenced by specific gravity, as higher specific gravity influences their thermal and mechanical properties [6].

Moreover, it can be observed from Fig.5 that Oyster shells exhibit an earlier onset and a sharper endothermic peak, indicating higher reactivity to thermal changes. In contrast, clam and scallop shells demonstrate delayed onsets and broader peaks, which shows slow heat transfer and decomposition. This behavior aligns with their steeper mass loss curve, as observed in the TGA data from Fig.3.

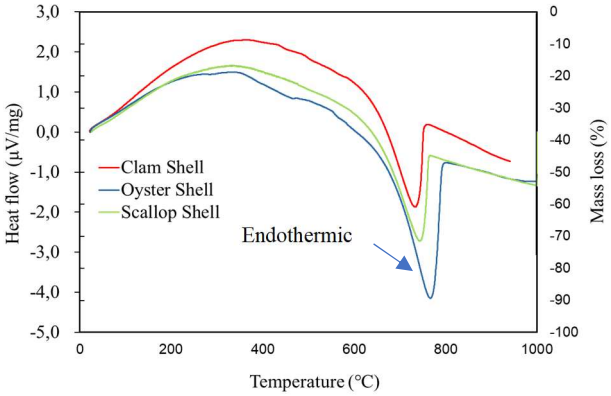

Fig.5 DTA Results for uncalcined sea shells

Furthermore, Fig.6 presents the TG-DTG and TG-DTA curves of sea shell samples subjected to calcination at 650 °C, 750 °C, and 850 °C. Across all samples, the curves exhibit similar trends, reflecting the thermal decomposition behavior of calcium carbonate ($CaCO_3$).

As an illustration, the TG-DTG analyses shown in Fig.6 (a) and (b) revealed the key insights into the decomposition of $CaCO_3$ during calcination. At 650 °C, the analyses indicate partial decomposition, resulting in a mixture of $CaCO_3$ and calcium oxide (CaO), indicating that the temperature was not sufficient for complete CaO conversion.

Subsequently, increasing the temperature to 750 °C promotes further decomposition, significantly reducing the residual $CaCO_3$ and increasing the proportion of CaO. Finally, at 850 °C, the calcination process nears completion, as indicated by the absence of residual $CaCO_3$ and minimal mass loss reduction, with nearly all $CaCO_3$ converted to CaO. This is further aligned with the XRD results in Fig.2 (b), (c), and (d), which depict a clear transition of $CaCO_3$ to CaO.

Meanwhile, the thermal decomposition of calcium hydroxide can be seen in Fig.6 (b), which is typically observed as a slight mass loss within the 400–500 °C [19]. This process corresponds to the decomposition reaction of $Ca(OH)_2$ into calcium oxide (CaO) and water vapor (H_2O).

Therefore, to preserve the purity of CaO after calcination, proper storage and handling are essential. Samples should be immediately placed in a vacuum chamber or sealed environment to prevent moisture absorption, which could lead to the reformation of calcium hydroxide. Existing studies have predominantly focused on specific temperature conditions (e.g., 750 °C) or limited their scope to a single type of seashell. In contrast, this research uniquely examines a broader range of temperature conditions and multiple seashell types, emphasizing its novelty and uniqueness.

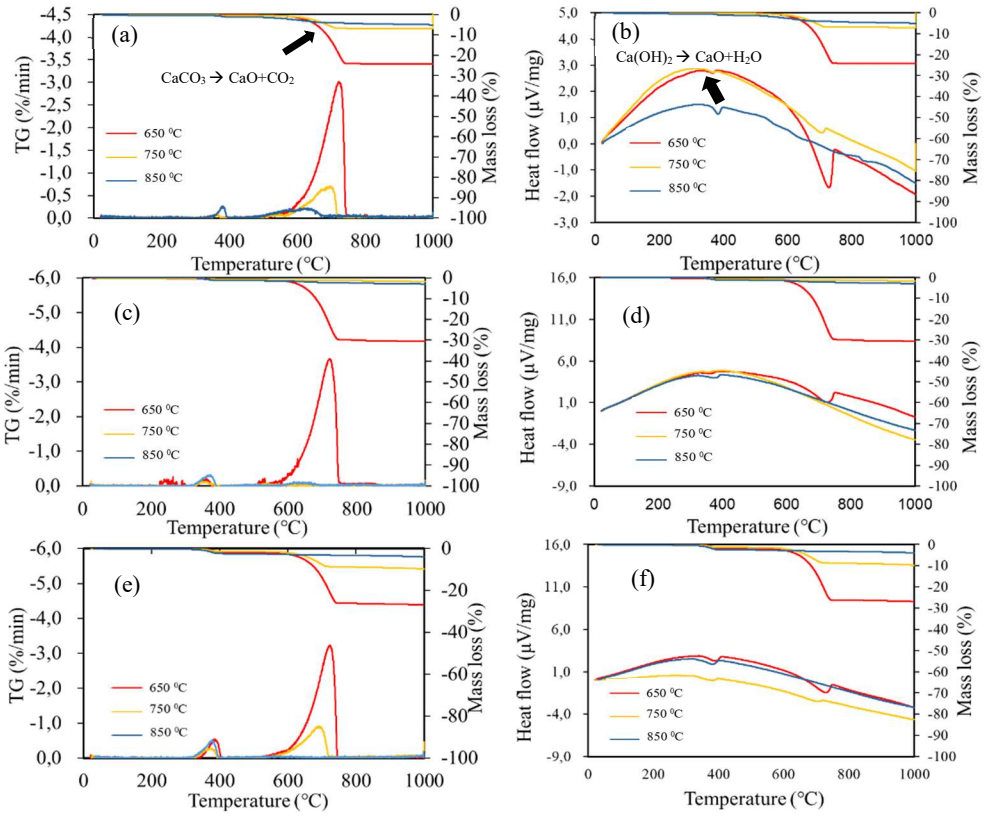

Fig.6 DTA Results for calcined (a) TG-DTG scallop shell, (b) TG-DTA scallop shell (c) TG-DTG oyster shell, (d) TG-DTA oyster shell, (e) TG-DTG clam shell, (f) TG-DTA clam shell

Ultimately, the decomposition of $CaCO_3$ (Fig.4) typically begins at 600°C to 800°C, with significant decomposition occurring at the optimum decomposition temperatures (ODT) for scallop, clam, and oyster shells of approximately 740°C, 730°C, and 750°C, respectively. Heating $CaCO_3$ beyond the ODT is unnecessary, as higher temperatures do not further enhance the decomposition process. Therefore, temperatures above the ODT increase energy consumption and carbon emissions, making them inefficient and unsustainable.

3.4 NMR results

The chemical shift in uncalcined scallops, oysters, and clam shells was investigated using solid-state NMR spectroscopy. Further, the ^{13}C NMR spectra, presented in Fig.7, were analyzed simultaneously with XRD data, offering complementary insights into the structural and chemical properties of the samples. In Fig.2, XRD analysis identified distinct crystalline phases, revealing that scallop and oyster shells are predominantly composed of calcite, while clam shells primarily consist of aragonite.

These findings were further confirmed by ^{13}C NMR spectroscopy, which detected similar chemical shifts characteristic of calcite at 168.19 ppm (CO_3^{2-}) and 168.20 ppm (CO_3^{2-}) in scallop and oyster shells and aragonite at 171.49 ppm (CO_3^{2-}) in clam shells, respectively. Notably, all samples exhibited carbonate peaks between 165–175 ppm, consistent with previous studies that identified chemical shifts indicative of $CaCO_3$.

A single peak at 168.21 ppm corresponds to calcite, while aragonite and vaterite exhibit peaks at 171.49 ppm and 170.12 ppm, respectively [5] [19]. In contrast to traditional XRD techniques, NMR spectroscopy offers numerous advantages. While XRD primarily identifies crystalline phases, NMR spectroscopy enables the detailed examination of carbonate ions, facilitates the differentiation of polymorphs, and detects poorly crystalline or amorphous phases [5]. Solid-state ^{13}C NMR spectra are an effective technique for distinguishing $CaCO_3$ polymorphs (aragonite, calcite, vaterite). Unlike XRD, which may struggle with peak overlaps in complex samples, ^{13}C NMR provides distinct chemical shifts for precise identification. It offers a more accurate characterization of seashell-derived $CaCO_3$ and its mineralogical properties.

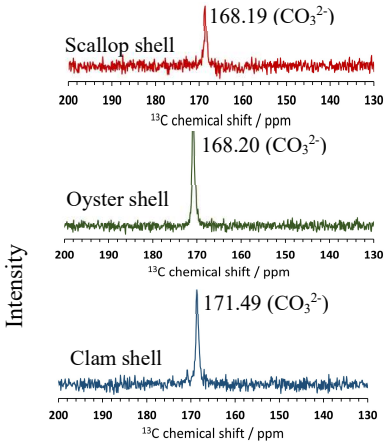

Fig.7 Results NMR of uncalcined sample

4. CONCLUSIONS

(1) TG-DTA results show that $CaCO_3$ decomposes between 600°C and 800°C, with optimum degradation temperatures (ODT) for scallop, clam, and oyster shells at 740°C, 730°C, and 750°C, respectively. In practical calcination process, exceeding this ODT limit may result in inefficient energy consumption and higher CO_2 gases.

(2) XRD and NMR analysis reveal distinct mineralogical compositions in samples, with scallop and oyster shells primarily containing calcite and clam shells containing aragonite.

(3) TGA patterns show three stages of weight loss, and Scallops and oyster shells exhibit the highest weight loss.

(4) NMR spectroscopy can detect $CaCO_3$, facilitate the differentiation of polymorphs, and detect poor crystalline phases. The ^{13}C NMR spectra were analyzed simultaneously with XRD data, offering complementary insights into the structural and chemical properties of the $CaCO_3$.

REFERENCES

[1] I. Imai *et al.*, "Prediction of toxic algal bloom occurrences and adaptation to toxic blooms to minimize economic loss to the scallop aquaculture industry in Hokkaido, Japan," *PICES Scientific Report* , vol. 47, 2014.

[2] H. Shimada, Y. Nishida, Y. Ito, and T. Mizushima, "Relationship among growth and survival of cultured scallops (Patinopecten yessoensis JAY), and environmental conditions in the coastal area off Yakumo, Funka Bay, Hokkaido, Japan. ," *Science Reports of Hokkaido Fisheries Experimental Station* , vol. 58, pp. 49–62, 2000.

[3] E. Haryati, K. Dahlan, O. Togibasa, and K. Dahlan, "The influence of calcination temperature to calcium content in the mangrove crab shells (Scylla serrata) from merauke," in *Journal of Physics: Conference Series*, IOP Publishing, 2021, p. 012024.

[4] K. H. Mo, U. J. Alengaram, M. Z. Jumaat, S. C. Lee, W. I. Goh, and C. W. Yuen, "Recycling of seashell waste in concrete: A review," *Constr Build Mater*, vol. 162, pp. 751–764, 2018.

[5] H. Nebel, M. Neumann, C. Mayer, and M. Epple, "On the Structure of Amorphous Calcium Carbonate□A Detailed Study by Solid-State NMR Spectroscopy," *Inorg Chem*, vol. 47, pp. 7874–7879, Jan. 2008, doi: 10.1021/ic8007409.

[6] Cinthya Alvarado and Hernán Alvarado-Quintana, "Thermal Decomposition of Seashell Powder," in *20th LACCEI International Multi-Conference for Engineering, Education, and Technology*, Boca Raton, Florida- USA, 2022.

[7] S. A. Rosli *et al.*, " Simple Thermal Treatment of Waste Oyster (Crassostrea belcheri) Shells for the Production of Calcium Minerals in Biomaterials Application ," *Nano Biomed Eng*, Mar. 2024, doi: 10.26599/nbe.2024.9290074.

[8] X. Inthapanya, S. Wu, Z. Han, G. Zeng, M. Wu, and C. Yang, "Adsorptive removal of anionic dye using calcined oyster shells: isotherms, kinetics, and thermodynamics," *Environmental Science and Pollution Research*, vol. 26, no. 6, pp. 5944–5954, 2019, doi: 10.1007/s11356-018-3980-0.

[9] K. Park, K. Sadeghi, and S. Thanakkasaranee, "Effects of calcination temperature on morphological and crystallographic properties of oyster shell as biocidal agent," *International Journal of Applied Ceramic Technology,* , vol. 18, no. 2, pp. 302–311, 2021.

[10] S. Seesanong *et al.*, "Economical and Environmentally Friendly Track of Biowaste Recycling of Scallop Shells to Calcium Lactate," *ACS Omega*, vol. 7, no. 17, pp. 14756–14764, May 2022, doi: 10.1021/acsomega.2c00112.

[11] N. Suwannasingha, A. Kantavong, S. Tunkijjanukij, C. Aenglong, H.-B. Liu, and W. Klaypradit, "Effect of calcination temperature on structure and characteristics of calcium oxide powder derived from marine shell waste," *Journal of Saudi Chemical Society*, vol. 26, no. 2, p. 101441, 2022.

[12] Candelario Ramón de los Santos *et al.*, "Effect of the thermal annealing on the phase transitions of biogenic CaCO3 nanostructures," *Mexican chemical society*, vol. 63, no. 2019, 2019.

[13] P. Ye, F. Xiao, and S. Wei, "Biomineralization and Characterization of Calcite and Vaterite Induced by the Fungus Cladosporium sp. YPLJS-14," *Minerals*, vol. 13, no. 10, Oct. 2023, doi: 10.3390/min13101344.

[14] S. Wu *et al.*, "Formation of stabilized vaterite nanoparticles via the introduction of uranyl into groundwater†," *Environ Sci Nano*, p., 2025, doi: 10.1039/D4EN00726C.

[15] 'Temperature and Free Energy.' Principles of Chemistry II, LibreTexts," Accessed January 7, 2025.

[16] E. Ferraz, J. A. F. Gamelas, J. Coroado, C. Monteiro, and F. Rocha, "Recycling Waste Seashells to Produce Calcitic Lime: Characterization and Wet Slaking Reactivity," *Waste Biomass Valorization*, vol. 10, no. 8, pp. 2397–2414, Aug. 2019, doi: 10.1007/s12649-018-0232-y.

[17] "TGA Plots Mass Loss Interpretation and ODT." Accessed: Feb. 10, 2025. [Online]. Available: https://www.lpdlabservices.co.uk/analytical_techniques/chemical_analysis/tga_interpret.php

[18] Seesanong S *et al.*, "Environmentally Friendly Track of Biowaste Recycling of Scallop Shells to Calcium Lactate.," vol. 2022.

[19] H. W. Papenguth, R. J. Kirkpatrick, B. Montez, and P. A. Sandberg, "13C MAS NMR spectroscopy of inorganic and biogenic carbonates," *American Mineralogist*, vol. 74, no. 9–10, pp. 1152–1158, 1989.